Inelastic Displacement Ratios of Smooth Hysteretic Behavior Systems subjected to Near-Fault and Far-Fault Earthquakes

Jong-Keol Song
Department of Civil Engineering, Kangwon National University, Chunchon 200-701, Korea

Kee-Jeung Hong
Department of Civil Engineering, Kookmin University, Seoul 136-702, Korea

15 WCEE
LISBOA 2012

SUMMARY:
In the performance-based design method, a peak displacement response is more important than traditional force-based design method. Peak displacement response is directly related to the damage state of inelastic structures. In order to control damage state of structures for various seismic design levels (or performance levels), the peak displacement response should be controlled in design process. Inelastic displacement ratio (IDR) is defined as the ratio of the peak inelastic displacement to the peak linear elastic displacement. IDR allows simple evaluation of the peak inelastic displacement directly from the peak elastic displacement without computation of inelastic response. Existing researches for the IDR are limited to the piece-wise linear systems such as the bilinear or the stiffness degrading systems. The actual hysteretic behavior of structural elements and systems is smooth. The smooth hysteretic behavior is more representative of actual behavior than piece-wise linear hysteretic models. By considering the effect of the smooth hysteretic behavior on the IDRs, accuracy of the inelastic displacement demand calculated from elastic displacement demand will be increased than existing formulas without smooth effects. In this paper, the IDR is investigated for the smooth hysteretic behavior systems subjected to the near- and far-fault earthquakes. The simple formula of the IDR is proposed by using the two step procedure of nonlinear regression analysis.

Keywords: Inelastic displacement ratio, smooth hysteretic behavior, near-fault earthquake, far-fault earthquake

1. INTRODUCTION

Seismic response prediction and seismic capacity evaluation, for new and existing structures subjected to strong ground motions, are a part of the most interesting research areas in the earthquake engineering. In the point of view of an inelastic response evaluation, many researchers recognize that performance-based seismic design method has more interesting concept than traditional force-based design method, because of peak displacement is used as main parameter in the performance-based seismic design method. Peak displacement response is directly related to the damage state of inelastic structures. In order to control damage state of structures for various seismic design levels (or performance levels), the peak displacement response should be controlled in design process.

The equal-displacement rule proposed by Veletsos and Newmark (1960) is described that the peak displacement of inelastic system is equal or less than the peak displacement of elastic system in the long period range. For oscillators with initial periods smaller than the characteristic period, T_g (Song and Pincheira, 2000), the inelastic displacements tended to be larger than the elastic displacements, depending on the strength or ductility of the system. The equal displacement approximation is generally applicable to stiffness- and strength degrading systems for periods greater than a characteristic period of the ground motion (Song and Pincheira, 2000). Peak displacements were generally larger than those of non-degrading systems (bilinear system) for periods less than T_g.

Inelastic displacement ratio (IDR) is defined as the ratio of the peak displacement of inelastic system to the peak displacement of elastic system. Existing researches (Song and Pincheira, 2000;

Ruiz-Garcia and Miranda, 2003a, 2006b; Hatzigeorgiou and Beskos, 2009; Mollaioli and Bruno, 2008; Hong and Jiang, 2004; Chopra and Chintanapakdee, 2004) for the IDR are limited to the piece-wise linear systems such as the bilinear or the stiffness degrading systems.

Since the actual hysteretic behavior of structural elements and systems is smooth, the smooth hysteretic behavior (Song and Gavin, 2011) is more similar to actual behavior than piece-wise linear hysteretic models. Therefore, an effect of smooth hysteretic behavior on IDRs is evaluated for near-fault and far-fault earthquakes. In this paper, a simplified and approximate formulation of the IDR considering the various smooth hysteretic characteristics and the near-fault effect of ground motions is proposed.

2. SDOF SYSTEM WITH SMOOTH HYSTERETIC BEHAVIOR

Inelastic behavior of the SDOF system subjected to ground motion ($\ddot{w}(t)$) can be described as the following equation (Song and Gavin, 2011),

$$\ddot{\mu}(t) + 2\xi\omega_n\dot{\mu}(t) + \omega_n^2((1-\alpha)z(t) + \alpha\mu(t)) = -\frac{\omega_n^2}{C_y g}\ddot{w}(t) \tag{2.1}$$

where, $\mu(t)$ is the ductility response, α is post-yield stiffness ratio defined as ratio of post-yield stiffness to elastic stiffness, C_y is a yield strength coefficient defined as the ratio of the yield force level to the weight of the system, and z(t) is normalized restoring force defined as the ratio of the inelastic restoring force to yield restoring force.

The normalized restoring force, z(t), obeys the following nonlinear differential equation using the Bouc-Wen model (Peng and Conte, 1997)

$$\dot{z}(t) = [\,1 - |z(t)|^p \,\mathrm{sgn}(\dot{\mu}(t)z(t))\,]\,\dot{\mu}(t) \tag{2.2}$$

where, p is the *smoothness exponent* in the hysteretic model. If $\dot{\mu}(\mathrm{t})z(\mathrm{t}) > 0$, $\mathrm{sgn}(\dot{\mu}(\mathrm{t})z(\mathrm{t}))$ is 1, otherwise, $\mathrm{sgn}(\dot{\mu}(\mathrm{t})z(\mathrm{t}))$ is -1.

The numerical solution (Song and Gavin, 2011) for smooth hysteretic behavior is developed using the Newmark-β approximations and Newton iterations. The algorithm (Song and Gavin, 2011) for constant-ductility response spectra is also developed using a combination of hyperbolic fits, the secant method, and Newton iterations. The numerical accuracy of the numerical solution for smooth hysteretic behavior and the algorithm for constant-ductility response spectra is verified by comparing strength-ductility relationship calculated by BiSpec (Hachem, 2004) and NONSPEC (Mahin and Lin, 1983) programs (Song and Gavin, 2011).

The effect of the smoothness exponent, p, defined in Equation (2.2), on the hysteretic behavior is shown in Figure 2.1. Values of p between 1 and 30 exhibit a range of hysteretic smoothness. Hysteretic behavior with p larger than 10 is similar to bi-linear behavior.

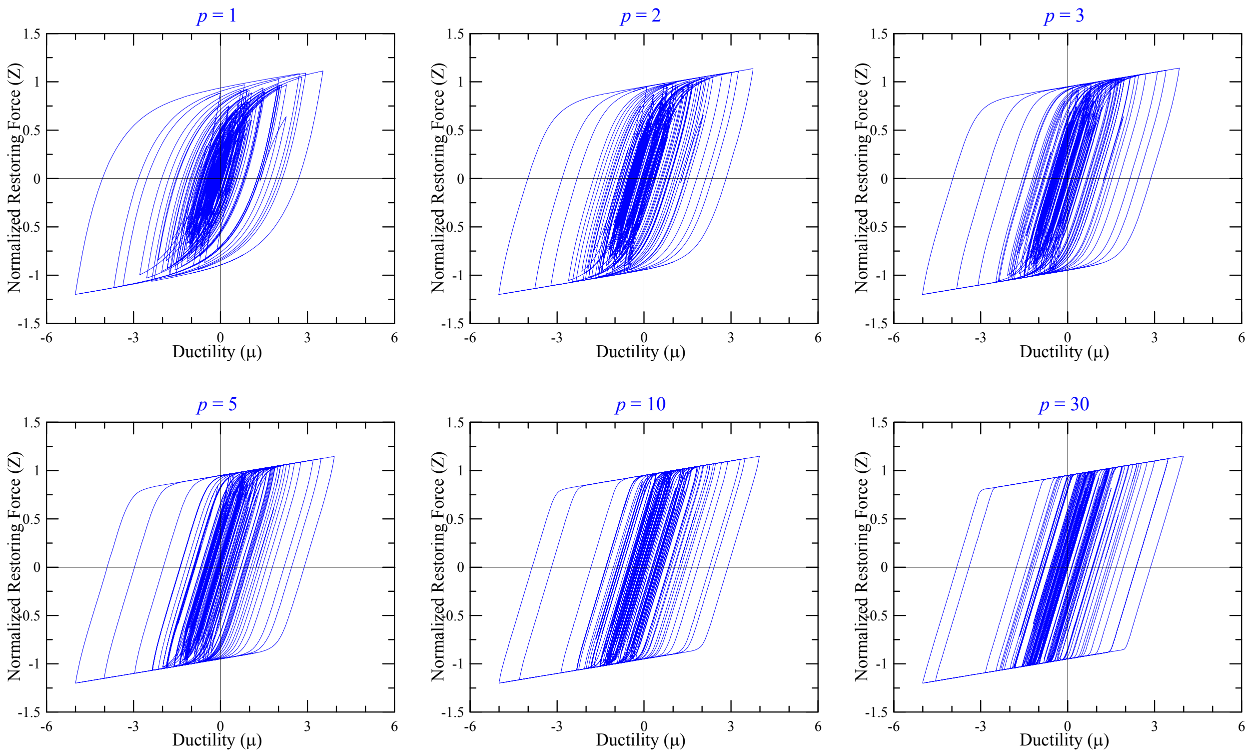

Figure 2.1. Effect of smoothness (p) on model hysteresis subjected to the SAC SE19 record (Vina del Mar, Chile, 1985) for SDOF oscillator with T_n = 1.0 sec, α =0.05, $\xi = 0.05$, and μ = 5 (the strength coefficients of each oscillator were adjusted independently to achieve a peak ductility of 5)

3. IDR FOR SDOF SYSTEM WITH SMOOTH HYSTERETIC BEHAVIOR

IDR, A_μ, is defined as

$$A_\mu = \frac{\max|r_{in}|}{\max|r_e|} \tag{3.1}$$

where, $\max|r_{in}|$ is maximum displacement of inelastic system and $\max|r_e|$ is maximum displacement of elastic system.

IDR, A_μ, is also derived from strength reduction factor (SRF), R_μ, defined as

$$R_\mu = \frac{\max|r_e|}{r_y} = \frac{\max|r_e|}{\max|r_{in}|}\mu = \frac{\mu}{A_\mu} \tag{3.2}$$

where, r_y is yield displacement of inelastic system.

Equation (3.2) is rewritten as

$$A_\mu = \frac{\mu}{R_\mu} \tag{3.3}$$

To propose a simple regression equation for IDR, 72 near-fault and 60 far-fault earthquakes are selected as shown in Tables 3.1 and 3.2. Details of earthquake records used, including earthquake names, magnitude, epicentral distance and peak ground acceleration (PGA), peak ground velocity (PGV) etc. are provided in the SAC steel project website (http://nisee.berkeley.edu/data/strong_motion/sacsteel/). Spectral displacements for the near-fault and far-fault earthquakes are compared in Figure 3.1. The mean spectral displacement for near-fault earthquakes is about twice than that of far-fault earthquakes.

Table 3.1. Far-fault ground motion records used in this study

NO.	SAC Name	Earthquake	Magnitude	Distance (km)	PGA (cm/sec^2)	PGV (cm/sec)
1	LA07	Landers, 1992, Barstow	7.3	36	412.98	66.08
2	LA08	Landers, 1992, Barstow	7.3	36	417.49	65.68
3	LA09	Landers, 1992, Yermo	7.3	25	509.70	91.31
4	LA10	Landers, 1992, Yermo	7.3	25	353.35	60.35
5	LA45	Kern, 1952	7.7	107	141.49	24.7
.	.	.	.	.	.	.
.	.	.	.	.	.	.
56	BO36	Saguenay, 1988	5.9	98	699.90	16.44
57	BO37	Saguenay, 1988	5.9	118	514.13	36.73
58	BO38	Saguenay, 1988	5.9	118	638.76	32.04
59	BO39	Saguenay, 1988	5.9	132	495.52	28.98
60	BO40	Saguenay, 1988	5.9	132	765.61	51.93

Table 3.2. Near-fault ground motion records used in this study

NO.	SAC Name	Earthquake	Magnitude	Distance (km)	PGA (cm/sec^2)	PGV (cm/sec)
1	LA01	Imperial Valley, 1940, El Centro	6.9	10	452.03	62.4
2	LA02	Imperial Valley, 1940, El Centro	6.9	10	662.88	59.9
3	LA03	Imperial Valley, 1979, Array #05	6.5	4.1	386.04	83
4	LA04	Imperial Valley, 1979, Array #05	6.5	4.1	478.65	48.19
5	LA05	Imperial Valley, 1979, Array #06	6.5	1.2	295.69	89.2
.	.	.	.	.	.	.
.	.	.	.	.	.	.
68	BO10	Nahanai, 1982	6.9	6.1	72.23	7.72
69	BO27	Nahanai, 1985 Station 1	6.9	9.6	246.99	10.74
70	BO28	Nahanai, 1985 Station 1	6.9	9.6	232.37	16.16
71	BO29	Nahanai, 1985 Station 1	6.9	6.1	170.20	21.03
72	BO30	Nahanai, 1985 Station 1	6.9	6.1	206.67	22.08

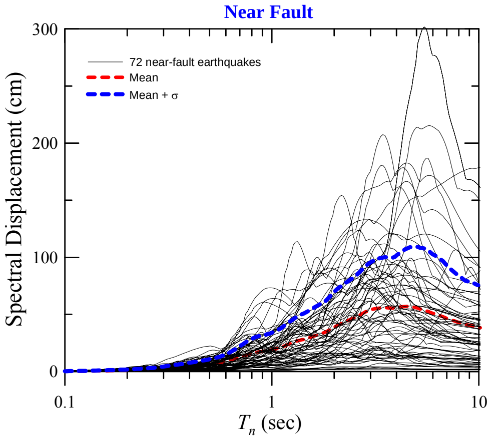

(a) near-fault earthquakes

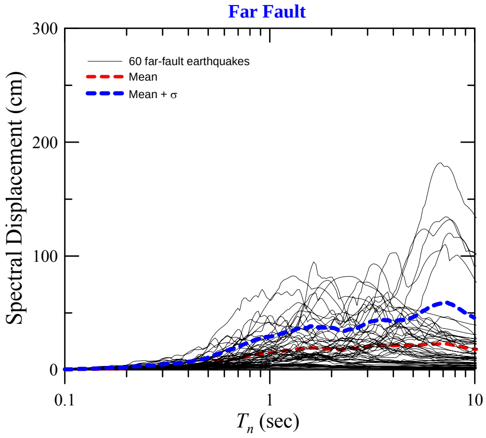

(b) far-fault earthquakes

Figure 3.1. Comparison of spectral displacements for near-fault and far-fault earthquakes

The influence of displacement ductility ratio (μ), defined as ratio of maximum displacement to yield displacement, on mean spectra of A_μ are evaluated for smooth hysteretic models (α=0, p=2 and 5% damping ratio) with various levels of μ for the 72 near-fault and 60 far-fault earthquakes, as shown in Figure 3.2. It can be observed that the A_μ increase with increasing μ. The A_μ spectra for the near-fault earthquakes and μ = 5 are larger than 1.0 for the period ranges less than about 1.5 seconds. The A_μ spectra for the far-fault earthquakes and μ = 5 are larger than 1.0 for the period ranges less than about 0.7 seconds. Figure 3.3 shows the coefficient of variation (COV) of A_μ spectra with several constant ductility values. It can be observed that the COV increase with increasing level of inelastic deformation with values varying from approximately 0.25 for μ =1.5 to approximately 0.4 for μ =10.

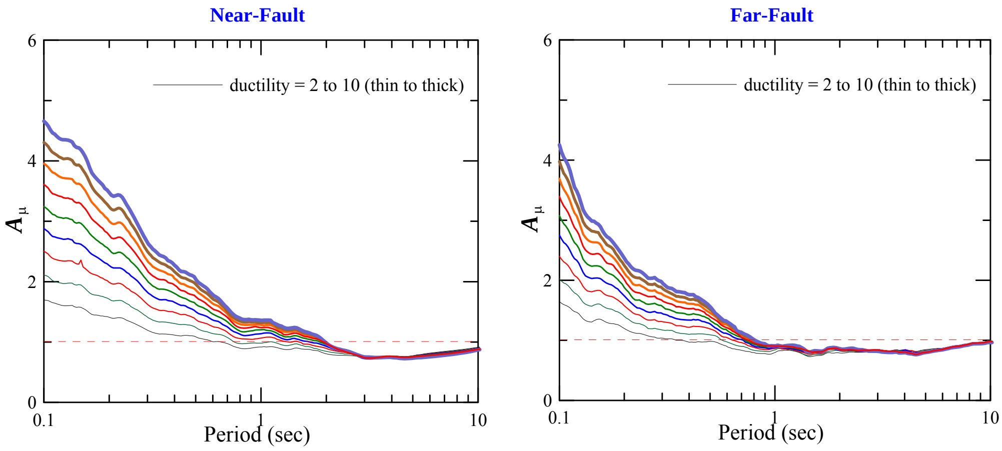

(a) near-fault (b) far-fault

Figure 3.2. Influence of μ on A_μ for smooth hysteretic model with α=0.0, p=1 and ξ =0.05

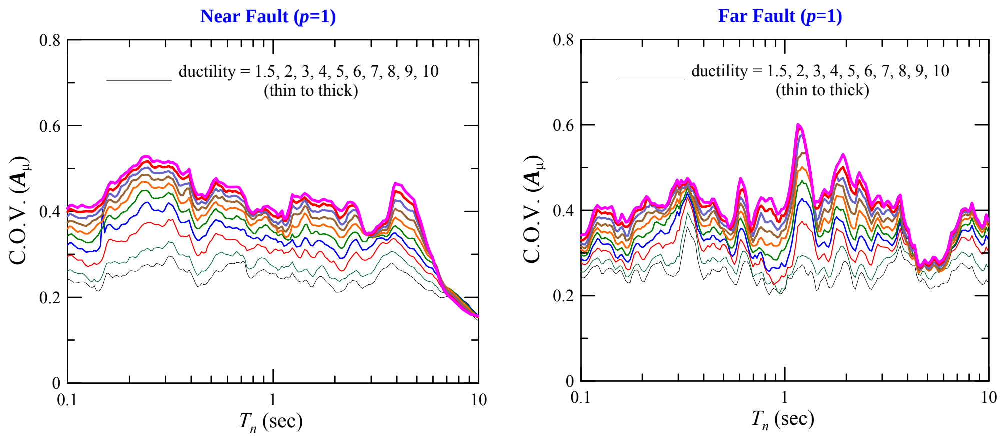

(a) near-fault (b) far-fault

Figure 3.3. Influence of μ on COV of A_μ for smooth hysteretic model with α=0.0, p=1 and ξ =0.05

The ratio (A_μ^{NF} / A_μ^{FF}) of IDR (A_μ^{NF}) for near-fault earthquakes to IDR (A_μ^{FF}) for far-fault earthquakes is compared in Figure 3.4. For the long period ranges larger than about 2.7 seconds, the values of A_μ^{NF} / A_μ^{FF} are less than 1, otherwise, the values of A_μ^{NF} / A_μ^{FF} are larger than 1. In other words, for the short period ranges less than about 2.7 seconds, A_μ^{NF} is larger than A_μ^{FF}, otherwise, opposite trend occurs. This trend can clear with increasing μ.

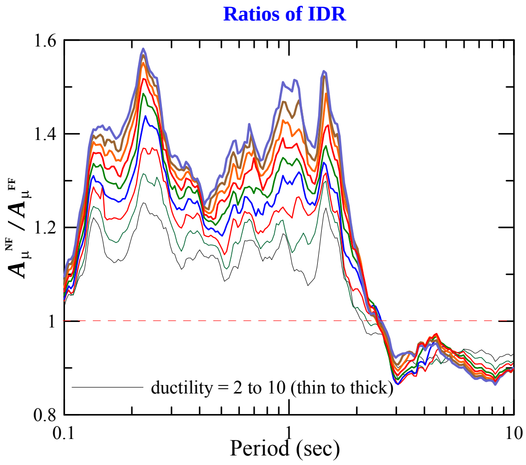

Figure 3.4. Comparison of the ratio (A_μ^{NF}/A_μ^{FF}) of IDR (A_μ^{NF}) for near-fault earthquakes to IDR (A_μ^{FF}) for far-fault earthquakes (α=0.0, p=1 and ξ=0.05)

IDR can be calculated from SRF using Equation (3.3). Since several equations for SRF were proposed by many researchers, the μ/R_μ may be easily calculated using the existing equations (Krawinkler and Nassar, 1992; Lai and Biggs, 1980; Newmark and Hall, 1973; Riddel, Hidalgo, and Cruz, 1989; Vidic, Fajfar, and Fischinger, 1992) for R_μ.

In order to evaluate an accuracy of A_μ calculated from R_μ, A_μ for near- and far-fault earthquakes are compared with μ/R_μ as shown in Figure 3.5. For μ =2, μ/R_μ is about 5% less than A_μ. For μ =10, μ/R_μ is about 15% less than A_μ. It means that the μ/R_μ can be underestimated about 5% ~ 15% than A_μ.

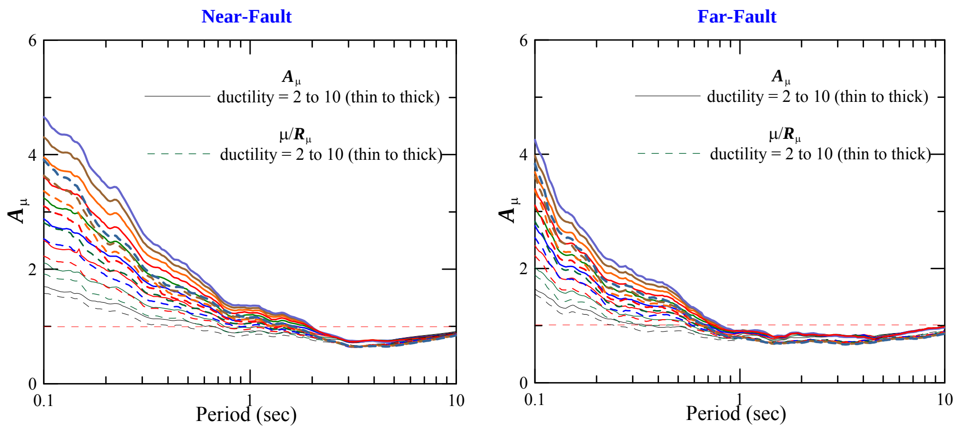

(a) near-fault (b) near-fault

Figure 3.5. Comparison of A_μ and μ/R_μ (α=0.0, p=1 and ξ=0.05)

Based on the observed dependency of the IDR with respect to the displacement ductility ratio, μ, and the period, T_n, an approximate formula for the IDR is function of μ and T. The effect of characteristics of the hysteretic smoothness and earthquakes for A_μ spectra are incorporated as recommended coefficients used in approximate formulation.

To develop an approximate formula for $A_\mu(T_n, \mu)$, a two-step nonlinear regression analysis is performed using mean values of A_μ spectra for various hysteretic smoothness (p=1, 2, 5, 10, 20, 100) models subjected to 72 near- and 60 far-fault earthquakes. One example of the regression analysis of $A_\mu(T_n, \mu)$, for the case of p=1 and far-fault earthquakes, is shown in Figures 3.6 and 3.7. In the first step as shown in Figure 3.6, the nonlinear regression for A_μ with variable T_n for discrete μ is carried out. In this figure, the solid lines represent the fitted curves by regression analysis and the solid lines with symbol represent real A_μ spectra. A simple regression equation for A_μ is proposed as shown in Equations (3.4) and (3.5). The A_μ of equation (3.4) has 1 for the elastic response (μ =1).

$$A_\mu = (\mu - 1)\Phi + 1 \tag{3.4}$$

$$\Phi = \frac{a}{\sqrt{1+T_n}} + \frac{b}{(1+T_n)^c} \tag{3.5}$$

where the coefficients *a*, *b,* and *c* can be obtained by the second step of the nonlinear regression analysis.

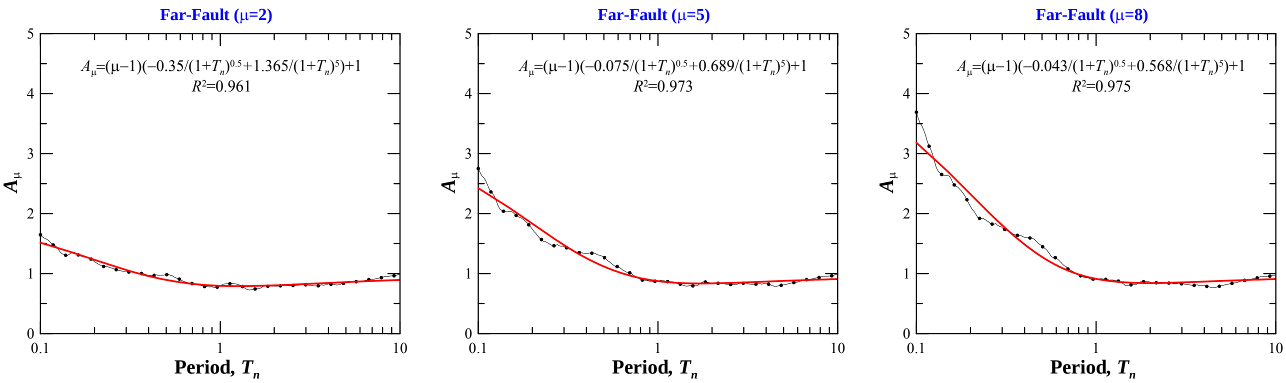

(a) μ =2 (b) μ =5 (c) μ =8

Figure 3.6. First-step of nonlinear regression analysis of A_μ for various ductility (case of far-fault earthquakes and *p*=1)

In order to evaluate the coefficients *a* and *b* of Equation (3.5), the second-step nonlinear regression analyses are performed as shown in Figure 3.7. Although the coefficients *a* and *b* are the function of μ, the coefficient *c* has almost constant value regardless of μ. Therefore, the coefficients *a* and *b* are evaluated from the nonlinear regression analysis using a properly assumed constant *c* (*c* = 4 for near-fault earthquakes, *c* =5 for far-fault earthquakes).

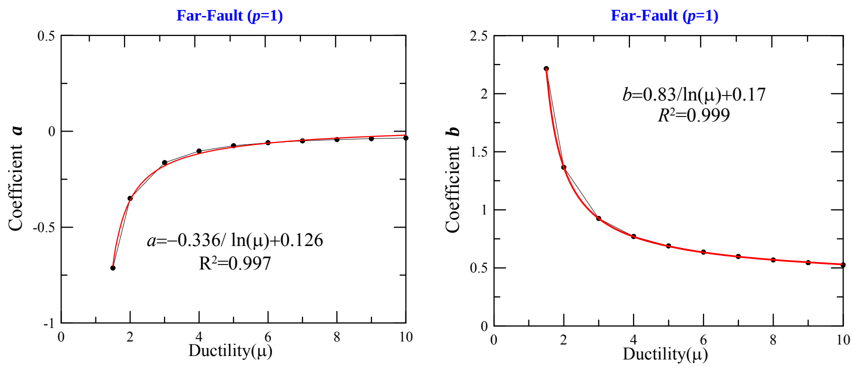

Figure 3.7. Second-step of nonlinear regression analysis of A_μ for various ductility (case of far-fault earthquakes and *p*=1)

For 12 cases made by combination of two earthquake types (near- and far-fault earthquakes), 6 smooth hysteretic models (*p*=1, 2, 5, 10, 20, and 100), the coefficients *a*, *b* and *c* of the Equation (3.5) are calculated using the two-step nonlinear regression analysis as shown in Table 3.3.

Table 3.3. Coefficients to compute A_μ with constant ductility for smooth hysteretic model

Earthquakes	Smoothness parameter (p)	a	b	c
Near-Fault	1	-0.345/ln(μ)+0.145	0.909/ln(μ)+0.224	4
	2	-0.311/ln(μ)+0.135	0.551/ln(μ)+0.352	4
	5	-0.213/ln(μ)+0.096	0.254/ln(μ)+0.477	4
	10	-0.158/ln(μ)+0.073	0.146/ln(μ)+0.524	4
	20	-0.124/ln(μ)+0.058	0.093/ln(μ)+0.548	4
	100	-0.075/ln(μ)+0.005	0.017/ln(μ)+0.639	4
Far-Fault	1	-0.336/ln(μ)+0.126	0.83/ln(μ)+0.17	5
	2	-0.292/ln(μ)+0.116	0.448/ln(μ)+0.285	5
	5	-0.202/ln(μ)+0.088	0.211/ln(μ)+0.367	5
	10	-0.144/ln(μ)+0.065	0.121/ln(μ)+0.403	5
	20	-0.102/ln(μ)+0.045	0.07/ln(μ)+0.428	5
	100	-0.042/ln(μ)-0.025	-0.026/ln(μ)+0.561	5

For the smooth hysteretic model with p=1, the approximate A_μ spectra obtained by the formulation proposed in this study are compared with real A_μ spectra calculated from numerical analysis as shown in Figure 3.8. It can be noted that real A_μ spectra are accurately fit by the approximate A_μ spectra. In other words, the approximate formulation can be used as a good tool for the IDR, if the coefficients of the approximate formulation are properly selected for structural behavior and characteristics of earthquakes. By selecting proper coefficients according to the hysteretic model and earthquakes type, the accuracy of the approximate formulation may be greater than the existing formulations, which do not consider the hysteretic and the earthquake characteristics.

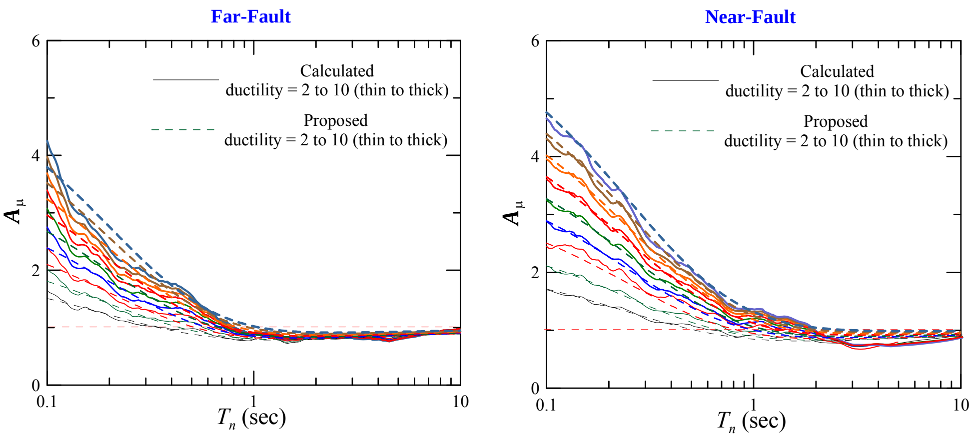

Figure 3.8. Comparison of A_μ estimated by the proposed regression equation and A_μ calculated from numerical analysis for various displacement ductility ratios (case of far-fault earthquakes and p=1)

4. CONCLUSIONS

This paper evaluates an IDR of smooth hysteretic behaviour systems subjected to near-fault and far-fault earthquakes. From the results obtained in this study, the following conclusions can be summarized as follows:

1. Simple and accurate formula for A_μ is proposed by two step nonlinear regression analysis, the formula includes two earthquake type (near- and far-fault earthquake) and six smooth hysteretic type (p=1, 2, 5, 10, 20, and 100). By considering the effect of the smooth hysteretic behavior on

A_{μ}, accuracy of the IDRs will be increased than existing formulas without smooth hysteretic effect.

2. In shorter periods than about 2.7 sec, A_{μ} for near-fault earthquakes has about 5~60% larger than A_{μ} for far-fault earthquakes. However, the opposite trend occurs in longer periods than about 2.7 seconds.

ACKNOWLEDGEMENT

This research was supported by Basic Science Research Program through the National Research Foundation of Korea (NRF) funded by the Ministry of Education, Science and Technology (2011-0010930). Additional funding was supported by the grant (2011T100100111) from the Ministry of Knowledge and Economy of Korean.

REFERENCES

Chopra, A.K. and Chintanapakdee, C. (2004). Inelastic deformation ratios for design and evaluation of structures: Single-degree-of-freedom bilinear systems. *Journal of Structural Engineering*, **130:9**, 1309-1319.

Hachem MM. (2004). Bispec: a nonlinear spectral analysis program that performs bi-direction dynamic time-history analysis of pendulum system. University of California at Berkeley, (http://nisee.berkeley.edu/elibrary/getpkg?id=BiSPEC).

Hatzigeorgiou, G.D. and Beskos, D.E. (2009). Inelastic displacement ratios for SDOF structures subjected to repeated earthquakes. *Engineering Structures*, **31**,2744-2755.

Hidalgo, P.A. and Arias, A. (1990). New Chilean code for earthquake-resistant design of buildings, *Proc. 4th U.S. Nat. Conf. Earthquake Engrg.*, Palm Springs, California. **2**,927-936.

Hong, H.P. and Jiang, J. (2004). Ratio between peak inelastic and elastic responses with uncertain structu ral properties. *Can. J. Civ. Eng.*, **31**,703-711.

Krawinkler, H. and Nassar, A. A. (1992). Seismic design based on ductility and cumulative damage demands and capacities, *Nonlinear Seismic Analysis and Design of Reinforced Concrete Buildings*, Elsevier Applied Science.

Lai, S.-P. and Biggs, J.M. (1980). Inelastic response spectra for aseismic building design, *J. Struct. Div., ASCE,* **106:ST6**,1295-1310

Mahin SA, Lin JP. (1983). Construction of inelastic response spectra for single-degree-of-freedom systems: computer program and applications. *Report UCB/EERC-83/17*, Earthquake Engineering Centre, University of California, Berkeley, CA. (http://nisee.berkeley.edu/elibrary/getpkg?id=NONSPEC).

Mollaioli, F. and Bruno, S. (2008). Influence of site effects on inelastic displacement ratios for SDOF and MDOF systems. *Computers and Mathematics with Applications*, **55**,184-207.

Newmark, N.M. and Hall, W.J. (1973). Seismic design criteria for nuclear reactor facilities, *Report No. 46, Building Practices for Disaster Mitigation*, National Bureau of Standards, U.S. Department of Commerce, pp. 209-236

Peng B.F. and Conte J.P. (1997). Statistical insight into constant-ductility design using a non-stationary earthquake ground motion model. *Earthquake Engineering and Structural Dynamics*, **26**,895-916.

Riddel, R., Hidalgo, P. and Cruz, E. (1989). Response modification factors for earthquake resistant design of short period structures. *Earthquake Spectra*, **5:3**,571-590.

Ruiz-Garcia, J. and Miranda, E. (2003). Inelastic displacement ratios for evaluation of existing structures. *Earthquake Engineering and Structural Dynamics*, **32**,1237-1258.

Ruiz-Garcia, J. and Miranda, E. (2006). Inelastic displacement ratios for evaluation of structures built on soft soil sites. *Earthquake Engineering and Structural Dynamics*, **35**,679-694.

Song, J.K. and Pincheira, J.A. (2000). Spectral displacement demands of stiffness- and strength-degrading systems. *Earthquake Spectra*, **16:4**,817-851.

Song, J.K. and Gavin, H.P. (2011). Effect of hysteretic smoothness on inelastic response spectra with constant-ductility. *Earthquake Engineering and Structural Dynamics*, **40**,771-788.

Vidic, T., Fajfar, P. and Fischinger, M. (1992). A procedure for determining consistent inelastic design spectra, *Proc. Workshop on Nonlinear Seismic Analysis of RC Structures*, Bled, Slovenia.

Veletsos, A.S. and Newmark, N.M. (1960). Effect of inelastic behavior on the response of simple systems to earthquake motions. *Proceedings of the 2nd World Conference on Earthquake Engineering*, **2**,895-912.